

**NOISE IN TRACKING RADARS**

**PART II**

**DISTRIBUTION FUNCTIONS  
AND FURTHER POWER SPECTRA**

A. E. Hastings, J. E. Meade, and H. L. Gerwin

Radio Division III

January 16, 1952



**APPROVED FOR PUBLIC  
RELEASE • DISTRIBUTION  
UNLIMITED**

**NAVAL RESEARCH LABORATORY**

**WASHINGTON, D.C.**

## CONTENTS

Abstract	ii
Problem Status	ii
Authorization	ii
INTRODUCTION	1
IMPROVEMENTS IN EQUIPMENT AND PRESENTATION	1
DATA	3
APPLICATION OF DATA TO RADARS	3
DISTRIBUTION FUNCTIONS	4
DISCUSSION	6
FUTURE WORK	6
APPENDIX A - Theory and Comparison of Methods of Obtaining Spectra	7
APPENDIX B - Curve Fitting by a Method of Least Squares	11

## ABSTRACT

Measurements of power spectra and distribution functions of radar echo fluctuation have been made on PB4Y and SNB airplanes. Data for angle of arrival and amplitude of the echo were obtained from the power spectra. The performance of a monopulse radar, under certain conditions, is superior to that of a sequentially-lobed radar.

## PROBLEM STATUS

This is an interim report on one phase of this problem; work is continuing.

## AUTHORIZATION

NRL Problem R12-13  
RDB Project NR 512-130

# NOISE IN TRACKING RADARS

## PART II - DISTRIBUTION FUNCTIONS AND FURTHER POWER SPECTRA

### INTRODUCTION

Sources and effects of noise in tracking radars were investigated previously.<sup>2,3</sup> The total tracking dispersion was divided into four components, each caused by an input noise: servo noise, receiver noise (thermal), amplitude noise (fluctuation in echo amplitude), or angle noise (fluctuation in echo angle of arrival). These components were compared qualitatively with varying target range. Equipment and tests were devised to obtain power spectra of angle noise and amplitude noise. Some quantitative data on amplitude noise and angle noise showed the effects of target size and type as well as of viewing angle.

In this earlier work, the ordinates  $A_{amp}$  of the spectra of amplitude noise were expressed as fractional modulation per  $\sqrt{\text{cps}}$  of bandwidth. Unity sinusoidal modulation was defined as the condition where the average echo level is equal to the peak of the sinusoidal modulating function. The ordinates  $A_{ang}$  of the spectra of angle noise were expressed in yards at the target per  $\sqrt{\text{cps}}$ . The output angular dispersion of a sequential radar due to amplitude noise is

$$\sigma_{amp} = 0.85 B A_{amp} \sqrt{\beta},$$

where  $A_{amp}$  is evaluated at the lobing frequency and is assumed constant over the range  $\pm\beta$ , the servo bandwidth, and where  $B$  is the beamwidth in mils of the antenna with parabolic lobe patterns having a crossover at 3 db (two-way pattern). The angular dispersion due to angle noise is

$$\sigma_{ang} = A_{ang} \sqrt{\beta/R},$$

where  $R$  is the target range and  $A_{ang}$  is assumed constant over the bandwidth 0 to  $\beta$ .

### IMPROVEMENTS IN EQUIPMENT AND PRESENTATION

Work on the problem has continued with improved equipment. An accurate method of angle calibration has been developed, using a movable beacon located near the ground. Triggered by a video pulse over a cable with the radar transmitter off, the beacon has

<sup>1</sup> This is Part II in a series of reports; Part I was NRL Report 3759, November 15, 1950, which gave preliminary data.

<sup>2</sup> Hastings, A. E., and Meade, J. E., "Improvement in Radar Tracking," NRL Report R-3424 (Confidential), February 24, 1949

<sup>3</sup> Meade, J. E., Hastings, A. E., and Gerwin, H. L., "Noise in Tracking Radars," NRL Report 3759 (Confidential), November 15, 1950

negligible leakage radiation, so that its antenna is essentially a point source. The method of obtaining the noise spectra from a repetitive sample of data has been given a new interpretation (Appendix A).

For convenient simulation, the noise spectra was represented by an analytic function corresponding to white noise through a realizable filter. Several spectra plotted with log-log coordinates were closely approximated by the transfer characteristics of a single-section RC low-pass filter. Accordingly, curves of the form

$$A_{\text{ang}} = A_{\text{ang}}(0) \left[ 1 + f^2/f_0^2 \right]^{-1/2}$$

have been fitted to the spectra of angle noise. Here  $f$  is frequency in cycles per second. Such a curve was superposed on the measured spectrum (Figure 1). Appendix B indicates how the parameters  $A_{\text{ang}}(0)$  (or  $a/b$ ) and  $f_0$  (or  $b$ ) are determined by a method of least squares. The total noise power in a bandwidth 0 to  $f_c$  is given by

$$P_c = \int_0^{f_c} A_{\text{ang}}^2(0) \left[ 1 + f^2/f_0^2 \right]^{-1} df = A_{\text{ang}}^2(0) f_0 \tan^{-1} f_c/f_0, \quad (1)$$

or for  $c$  with large value, by

$$P_c = \frac{\pi}{2} A_{\text{ang}}^2(0) f_0. \quad (2)$$

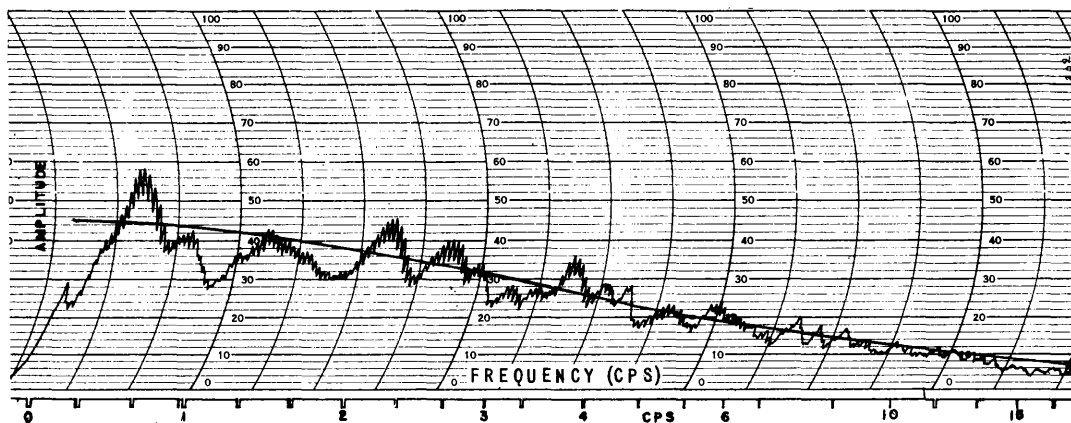


Figure 1 - Amplitude-frequency spectrum and approximating smooth curve for angle noise for SNB at  $0^\circ$  in train

The development of a distribution analyzer<sup>4</sup> has made it possible to calculate rapidly the amplitude distribution of amplitude noise and of angle noise. The analyzer plots the probability that the amplitude of a function will lie in a narrow range,  $\Delta e$ , against  $e$ . Samples of noise, recorded on a loop of magnetic tape and repeated while the analyzer slowly scans the resulting time function, provided distribution curves. From the first moment of such a curve, can be obtained the average center of reflection relative to the beacon on the target. When the beacon is on one end of the target, a rough check on the radar calibration is available, since it is known that the average center of reflection is near the geometrical center. The second moment of the distribution curve is the total power, which can be compared with that obtained from the power spectrum for the same upper-frequency limit  $f_c$ .

<sup>4</sup> King, A. M., "A Distribution Analyzer," NRL Report 3890, January 1952

## DATA

Test runs have been repeated on two aircraft of widely differing dimensions, an SNB and a PB4Y. A number of recordings of angle noise were made for each of three plane aspects. The values  $A_{ang}(0)$  and  $f_0$  were determined for each run and averaged. These averages, the rms deviations of the individual runs, and the resulting  $\sigma_{ang}$  for a radar with a servo passband of 1/2 cps are shown in Table 1. The values  $A_{amp}(30)$  and  $\sigma_{amp}$  are those previously published for such a radar with sequential lobing rate of 30 cps and beamwidth 30 mils. At the range  $R_0$ , the angle and amplitude effects are equal.

Spectra of amplitude noise in a passband similar to that for angle noise, 0.01 to 15 cps, have been obtained from runs on the SNB. These are similar to the spectra of angle noise and can be approximated as well by the RC filter characteristic, with about the same value of  $f_0$ . Spectra of amplitude noise for frequencies up to 500 cps have been published previously<sup>5</sup> and show a continuation of the slope of the low-frequency spectra.

TABLE 1  
Noise and Dispersion Data for SNB and PB4Y Airplanes

Airplane	Angle	Aspect ( $^{\circ}$ )	$A_{ang}(0)$	$f_0$ (cps)	$\sigma_{ang}$ (mils)	$A_{amp}(30)$	$\sigma_{amp}$ (mils)	$R_0$ (yd)
SNB	Train	0	2.3	1.3	1600/R	$2.0 \times 10^{-2}$	0.36	4500
SNB	Train	90	2.7	2.3	1900/R	$2.3 \times 10^{-2}$	0.41	4600
SNB	Train	180	3.3	2.4	1800/R	$1.2 \times 10^{-2}$	0.22	8200
SNB	Elevation	0	1.4	0.9	1000/R	$2.0 \times 10^{-2}$	0.36	2800
SNB	Elevation	90	1.8	1.0	1300/R	$2.3 \times 10^{-2}$	0.41	3200
SNB	Elevation	180	2.0	1.5	1200/R	$1.2 \times 10^{-2}$	0.22	5500
PB4Y	Train	0	1.4	1.6	1000/R	$1.4 \times 10^{-2}$	0.25	4000
PB4Y	Train	90	3.0	1.7	2100/R	$0.8 \times 10^{-2}$	0.14	15000
PB4Y	Train	180	3.0	1.4	2100/R	$0.6 \times 10^{-2}$	0.11	19000
PB4Y	Elevation	0	0.7	1.7	500/R	$1.4 \times 10^{-2}$	0.25	2000
PB4Y	Elevation	90	0.8	1.9	600/R	$0.8 \times 10^{-2}$	0.14	4300
PB4Y	Elevation	180	0.9	1.6	600/R	$0.6 \times 10^{-2}$	0.11	5500

## APPLICATION OF DATA TO RADARS

The application of this data to a sequentially lobed radar such as the Mark 25 Mod 6, with servo passband 1/2 cps and antenna beamwidth 30 mils, leads to some interesting conclusions. For an average airplane target, an SNB with side view ( $90^{\circ}$ ), the output dispersion due to amplitude noise would be 0.46 mil and independent of range  $R$ . The servo noise of the Director Mark 37 has been quoted as 0.25 mil. The dispersion due to angle noise is given by  $1900/R$ , and receiver noise is assumed negligible. These dispersions add in rms fashion, giving the total noise (Figure 2). The dispersion is also shown for a servo noise of 0.1 mil and for a monopulse radar with the same characteristics but inherently not affected by amplitude noise. These results should be used with caution, since all the components are subject to considerable fluctuation. However, they do serve to establish design parameters. The curves presented would perhaps justify the use of a monopulse system for operation at the longer ranges.

<sup>5</sup> See footnote 3

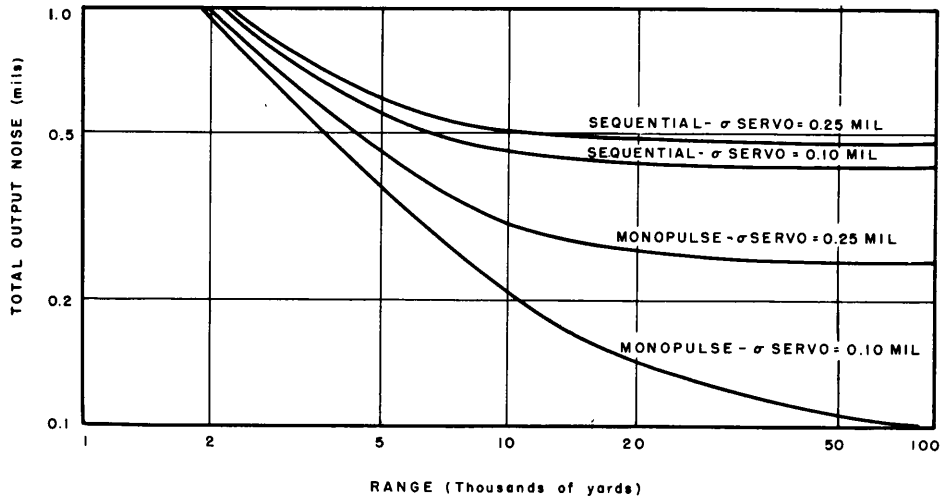


Figure 2 - Total output dispersion of sequential and monopulse radars (typical, but data varies greatly)

DISTRIBUTION FUNCTIONS

A study has been made of the distribution functions of echo amplitude noise from various aspects of an SNB airplane. Since the passband that can be recorded is limited, the noise was studied in two regions — from 0.01 to 15 cps and from 0.2 to 500 cps. In Figure 3, a Gaussian function with the same rms and average values and the same area under the curve is superposed on a distribution curve for the high-frequency region. All the distributions obtained in this region approximate the Gaussian function, although occasional ones show slightly skewed or double-humped shapes. The distributions obtained in the low-frequency region are not so closely Gaussian as those in the high-frequency region, but tend toward the Rayleigh form (Figure 4).

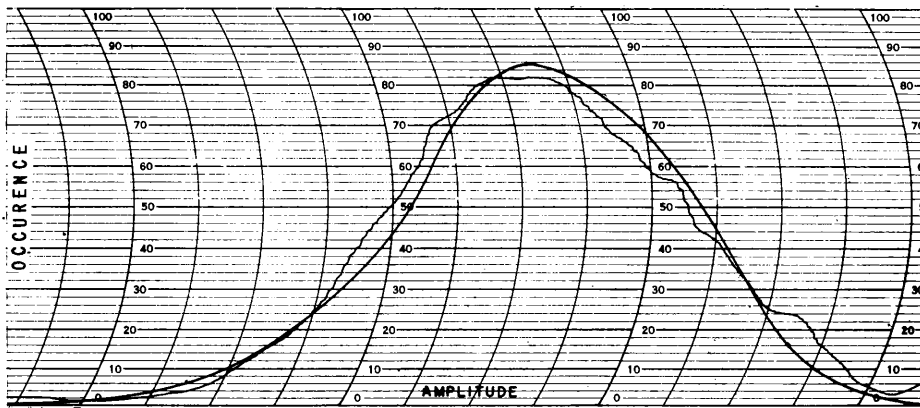


Figure 3 - Distribution of amplitude noise with superposed Gaussian (smooth curve) for SNB at 0° with a passband of 0.2 to 500 cps

A qualitative explanation of these results can be made on the basis of some published studies<sup>6</sup> of the detection of a sine wave plus noise. For noise alone, the distribution of detector output is of Rayleigh form, as would occur if an airplane target were a completely

<sup>6</sup>Rice, S. O., "Mathematical Analysis of Random Noise," Bell System Tech. Jour. 24, p. 102, January 1945

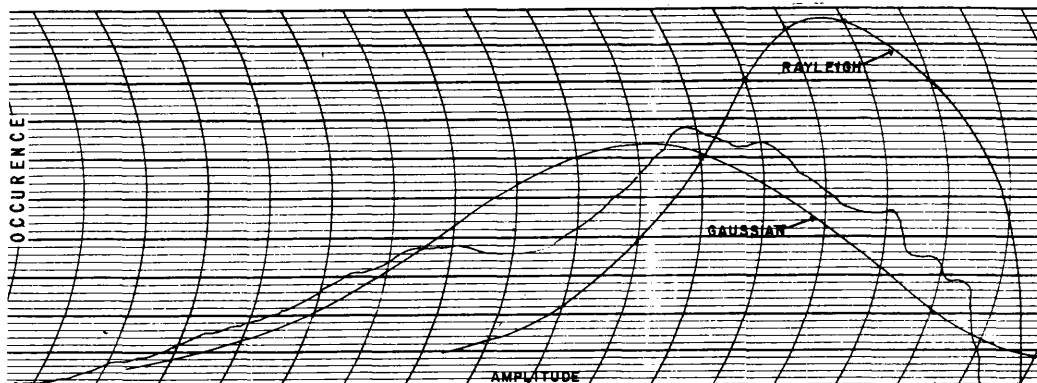


Figure 4 - Distribution of amplitude noise with superposed Gaussian and Rayleigh functions for SNB at  $90^\circ$  with a passband of 0.01 to 15 cps

random scatterer. As the scattering becomes more coherent, causing a sine-wave carrier plus sideband noise, the distribution approaches a Gaussian form. For the low-frequency region, 0.01 to 15 cps, the target is then partly coherent and partly random in its scattering. If band limiting occurs after detection, the otherwise Rayleigh form also approaches the Gaussian. This could explain the Gaussian form for the high-frequency region, where, although the passband is quite wide, the noise spectrum peaks at low frequencies so that the effect is that of a smaller passband.

A similar study of the distribution of angle noise has been made. From calibration data, the abscissas of the distribution functions are expressed directly in yards at the target, and the airplane dimension can be drawn in (Figure 5). The point of average echo return is roughly at the center and the apparent source is at times outside the airplane. The smooth line is the equivalent Gaussian curve. The total noise in a passband from 0 to 17 cps has been computed for the angle noise recorded from several runs (Table 2). In the second column this noise is calculated by Equation (2) from the spectra and in the third column from the second moment of the distribution curve. The means of these two columns agree very well. The fourth column, from the first moment of the distribution curve, gives the distance from the beacon to the center of reflection and is about half the length of the airplane.

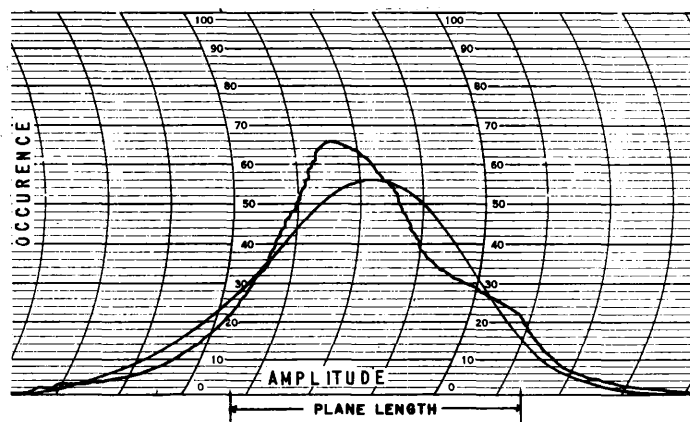


Figure 5 - Distribution of angle noise with superposed Gaussian (smooth curve) for SNB at  $0^\circ$  in train with a passband of 0.01 to 15 cps

TABLE 2

Angle-Noise Power and Center of Reflection for SNB Airplane			
Run	Spectrum (yd <sup>2</sup> /cps)	Distribution (yd <sup>2</sup> /cps)	Beacon to Center of Reflection (yd)
302	5.0	4.1	5.6
303	4.4	5.4	6.8
304	5.2	4.9	7.0
305	3.8	4.1	4.9
311	4.9	3.0	8.0
312	6.3	7.6	2.3
Mean	4.93 ± 0.8	4.85 ± 1.4	5.77 ± 1.8

## DISCUSSION

Some measurements made with two airplane targets closely spaced produced spectra essentially the same as obtained from a single target except in magnitude. Most of the distribution curves are closely Gaussian, but a few are skewed or double-humped.

The data in Table 1 indicate about the same values of angle noise for the SNB and PB4Y airplanes. Since the PB4Y has about twice the dimensions of the SNB, there is no apparent correlation of measured noise with airplane size. This is in contrast to the data for either airplane alone, in which the smaller vertical airplane dimension agrees with the smaller noise values in elevation. Without data on other types of airplanes, there seems no explanation of this at present.

Measurements have been made of amplitude noise from a F94 jet airplane made available by the Air Force.  $A_{amp}(30)$  is somewhat lower on the average than the values in Table 1, and the amplitude-frequency spectra show less noise at high frequencies. These differences may be the result of more rigidity and more streamlining in the design of the jet airplane.

Some of the data in Table 1 have been checked closely by additional tests at various intervals of time. The probable error is thought to be within the fluctuation of the data. The data analyzing system is linear within a few percent, and the radar is operated within the approximately linear region of its antenna pattern.

## FUTURE WORK

Additional work planned will include further measurements on a jet airplane and on two airplanes closely spaced. Range noise, which is receiving preliminary study with recently completed instrumentation, will be investigated in some detail.

\*\*\*

APPENDIX A  
THEORY AND COMPARISON OF METHODS OF OBTAINING SPECTRA

A previous report<sup>1A</sup> described the general problems of obtaining amplitude frequency spectra from a recorded time function. A later report<sup>2A</sup> described the spectra of echo amplitude noise obtained by a method somewhat different from that used in the present report. The theory is repeated with a simpler presentation and a more complete interpretation.

THEORY OF THE METHODS

Assume first a periodic time function with a single frequency component of period  $T_1$ , amplitude  $A$ , and phase angle  $\phi$ , given by

$$f_1(t) = A \sin(2\pi t T_1^{-1} + \phi).$$

A piece of  $f_1(t)$  is chosen of duration  $mT_1$ , so that  $m$  represents the number of periods of  $f_1(t)$  chosen,  $m$  not being restricted to integral values. Let  $T = mT_1$  and expand  $f_1(t)$ . Then over the interval  $-T/2$  to  $T/2$

$$f_1(t) = A \left[ \sin 2\pi m t T^{-1} \cos \phi + \cos 2\pi m t T^{-1} \sin \phi \right] \quad (1A)$$

If  $f_1(t)$  is expanded in a Fourier series over the limits  $-T/2 < t < T/2$ ,

$$\begin{aligned} f_1(t) &= a_0/2 + \sum_{n=1}^{\infty} a_n \cos 2\pi n t T^{-1} + \sum_{n=1}^{\infty} b_n \sin 2\pi n t T^{-1} \\ &= a_0/2 + \sum_{n=1}^{\infty} c_n \sin(2\pi n t T^{-1} + \tan^{-1} a_n b_n^{-1}), \end{aligned} \quad (2A)$$

where  $c_n^2 = a_n^2 + b_n^2$ . Here  $a_0$  is of no interest, and  $a_n$  and  $b_n$  are given by

$$a_n = \frac{2}{T} \int_{-T/2}^{T/2} f_1(t) \cos 2\pi n t T^{-1} dt,$$

and

$$b_n = \frac{2}{T} \int_{-T/2}^{T/2} f_1(t) \sin 2\pi n t T^{-1} dt.$$

<sup>1A</sup> Hastings, A. E., "Methods of Obtaining Amplitude-Frequency Spectra," NRL Report R-3466 (Unclassified), 16 May 1949

<sup>2A</sup> Hastings, A. E., "Amplitude Fluctuation in Radar Echo Pulses," NRL Report R-3487 (Confidential), 21 June 1949

If  $f_1(t)$  from Equation (1A) is substituted in the above equations and the integration carried out,

$$a_n = \left[ \frac{\sin(m+n)\pi}{(m+n)\pi} + \frac{\sin(m-n)\pi}{(m-n)\pi} \right] A \sin \phi,$$

$$b_n = \left[ -\frac{\sin(m+n)\pi}{(m+n)\pi} + \frac{\sin(m-n)\pi}{(m-n)\pi} \right] A \cos \phi,$$

and

$$c_n^2 = A^2 \left[ \frac{\sin(m+n)\pi}{(m+n)\pi} + \frac{\sin(m-n)\pi}{(m-n)\pi} \right]^2$$

$$- 4A^2 \frac{\sin(m+n)\pi}{(m+n)\pi} \frac{\sin(m-n)\pi}{(m-n)\pi} \cos^2 \phi.$$

The selected piece of  $f_1(t)$  is defined by Equation (2A) over the restricted interval  $-T/2$  to  $T/2$ . If this piece is repeated with the period  $T$ , a new periodic function results, defined as  $f(t)$  and given by Equation (2A) with  $t$  unrestricted to any interval. The component amplitudes of  $f(t)$  are given by  $c_n$  and the component periods by  $T/n$ . It is of interest to determine what information about the spectrum of the original time function  $f_1(t)$  can be obtained from the discrete spectrum of  $f(t)$ . Three cases occur.

I.  $m = n$ . Then a whole number of periods of  $f_1(t)$  have been chosen for repetition and, regardless of the values of  $m$  and  $\phi$ , an analyzer exploring the spectrum of  $f(t)$  finds only one value of  $c$ , that when  $m = n$ , where  $c = A$ , the required amplitude of the original time function.

II.  $m \neq n$  and  $n \gg 1$ . Here many periods of  $f_1(t)$  are chosen for repetition. The variation of  $c_n/A$  is shown in Figure 1A for  $n = 10$  and  $n = 100$ . Then  $c_n$  is small except for values of  $n$  close to  $m$ , is independent of  $\phi$ , and is given by

$$c_n = A \frac{\sin(m-n)\pi}{(m-n)\pi}.$$

Then

$$f(t) = a_0/2 + \sum_{n=1}^{\infty} c_n \sin(2\pi n t/T + \phi).$$

An analyzer finds only a few major values of  $c_n$  with periods differing by  $T$ . If at least five of the components of  $f(t)$  around  $m = n$  are included in the analyzer bandwidth, the rms value of the five is always within a few percent of  $A$ . If, however, the analyzer bandwidth includes only one component, the indicated value of  $c_n$  varies from 0 to  $A$ , depending on the value of  $m$ . If various lengths of  $f_1(t)$  are chosen, some indication of the maximum value of  $c_n = A$  is given.

III.  $m \neq n$  and  $n$  is small. Then  $c_n$  depends on  $\phi$  as well as on  $m$ , as shown in Figure 1A for  $n = 1$ ,  $\phi = 0$ . Only by choosing both  $n$  and  $\phi$  within close limits can  $c_n$  approximate to the value of  $A$ .

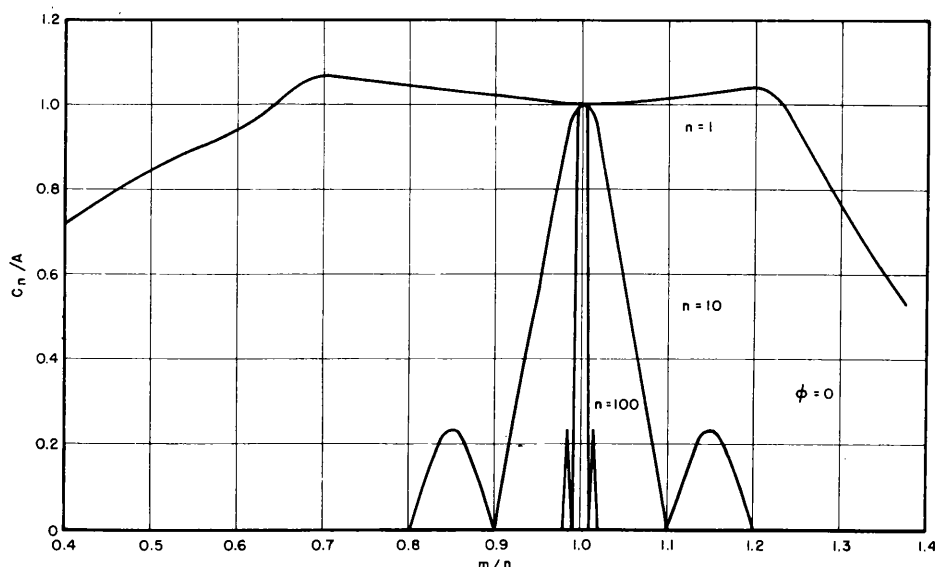


Figure 1A - Resolving power of the analyzer

Figure 1A also indicates the resolving power of the process. Suppose  $f_1(t)$  includes two components with equal amplitude and with frequencies close together, such that  $m = n$  for one and  $m$  approaches  $n$  for the other. The resolving power, defined as the separation of frequencies so that one is indicated as a maximum and the other at the first null, is 10 percent for  $n = 10$  and 1 percent for  $n = 100$ . It is assumed that the analyzer that was used includes only one component in its bandwidth, which makes the determination of  $A$  uncertain. The optimum bandwidth involves, then, a compromise between resolving power and accuracy of indication.

If  $f_1(t)$  is a complex function, with more than one frequency component,  $m$  has a number of values. If  $f_1(t)$  is nonperiodic,  $m$  becomes a continuous variable, and the amplitude of  $f_1(t)$  is a function of  $m$ . Let  $A^2(m)$  be the power in a bandwidth  $dm$  and  $A^2(m)$  vs.  $m$  the desired power spectrum. If  $n$  is restricted to large values, the discrete spectrum  $f(t)$  has the amplitude  $c_n$  given by

$$c_n^2 = \int_0^{\infty} A^2(m) \left[ \frac{\sin(m-n)\pi}{(m-n)\pi} \right]^2 dm.$$

But  $\frac{\sin(m-n)\pi}{(m-n)\pi}$  is very small except over a small interval of  $m$ , so that most of the contribution to the integral occurs over this interval. If  $A^2(m)$  is restricted to a continuous function which changes slowly with  $m$ ,  $A^2(m)$  can be considered constant within this interval and can be taken outside of the integral. Then

$$c_n^2 = A^2(m) \int_0^{\infty} \left[ \frac{\sin(m-n)\pi}{(m-n)\pi} \right]^2 dm = \frac{\pi}{2} A^2(m).$$

Then,  $A(m) = \sqrt{2/\pi} c_n$ , and the amplitude of the continuous spectrum  $A(m)$  of  $f_1(t)$  is given by the amplitude of the  $n$ th harmonic of the periodic function  $f(t)$ . If the analyzer bandwidth

includes several components of  $f(t)$ , the analyzer indication is a continuous representation of  $A(m)$ .

Since the phase of the data sample is unimportant ( $n \gg 1$ ), only one sample, if representative, should give the correct shape of the spectrum. If one sample is not representative, an average of several samples of equal length is desirable. A geometric average is preferable, since it will give the correct spectrum shape independent of any over-all changes of magnitude in the samples.

#### COMPARISON OF METHODS

The first measuring arrangement employed a transfer of the time function to an opaque rotating circular plot. The amplitude of the original function, proportional to the plot radius, modulated a light source falling on a photocell. A wave analyzer indicated the amplitudes  $c_n$  in the photocell current.  $T$  was  $1/30$  second, and the harmonics were spaced over 30-cps intervals, while the bandwidth of the analyzer was 4 cps. As predicted by the theory (Case II), there was considerable scatter of the amplitudes  $c_n$  in each sample and from sample to sample. The average of several samples gave the generally decreasing amplitude with frequency described in the present report, but the resolving power was too low to indicate periodic components of propeller modulation. In the work now continuing,  $T \cong 3$  seconds, the harmonics are spaced over  $1/3$ -cps intervals, and the analyzer always includes a number of them in its bandwidth. The improved resolving power and smoothness of data are evident in the spectra.

\*\*\*

APPENDIX B  
CURVE FITTING BY A METHOD OF LEAST SQUARES

The assumed curve is of the form

$$y = a(b^2 + x^2)^{-1/2}.$$

The method of least squares requires the minimization of

$$\sum_i \left[ y_i - a(b^2 + x_i^2)^{-1/2} \right]^2,$$

where the  $y_i$ 's are the observed values. The partial derivatives with respect to  $a$  and  $b$  are equated to zero, giving

$$\sum_i y_i (b^2 + x_i^2)^{-1/2} = a \sum_i (b^2 + x_i^2)^{-1},$$

and

$$\sum_i y_i (b^2 + x_i^2)^{-3/2} = a \sum_i (b^2 + x_i^2)^{-2}.$$

Elimination of  $a$  can be accomplished by equating the quotient of the left-hand terms to that of the right-hand terms. However, the resulting equation cannot be solved explicitly for  $b$ . If the value of

$$D = \frac{\sum_i y_i (b^2 + x_i^2)^{-1/2}}{\sum_i y_i (b^2 + x_i^2)^{-3/2}} - \frac{\sum_i (b^2 + x_i^2)^{-1}}{\sum_i (b^2 + x_i^2)^{-2}}$$

is found for two values of  $b$ , the true value of  $b$  for  $D = 0$  can be found by linear interpolation. Values of  $b$  should preferably be chosen to make  $D$  positive for one and negative for the other. If the terms in parentheses and the right-hand quotient are calculated for several standard values of  $b$ , the remaining calculations for each curve are rather simply carried out on a computing machine. Calculation of  $a$  by either,

$$a = \frac{\sum_i y_i (b^2 + x_i^2)^{-1/2}}{\sum_i (b^2 + x_i^2)^{-1}},$$

or

$$a = \frac{\sum_i y_i (b^2 + x_i^2)^{-3/2}}{\sum_i (b^2 + x_i^2)^{-2}},$$

could be made from the true value of  $b$ , but an interpolation is simpler, since the sums are already calculated. For each value of  $b$  assumed, values of  $a$  calculated from both equations are arbitrarily averaged. A linear interpolation between the averages gives  $a$  for the true  $b$ . Curves obtained by this method for  $y_i$ 's calculated from the assumed formula give very satisfactory approximations.

\*\*\*